

# Particle Acceleration and Gamma-Ray Production in Shell Remnants

H.J.Völk

*Max-Planck-Institut für Kernphysik, Heidelberg, Germany*

## Abstract

A number of nearby Northern Hemisphere shell-type Supernova Remnants (SNRs) has been observed in TeV  $\gamma$ -rays, but none of them could be detected so far. This failure calls for a critical reevaluation of the theoretical arguments for efficient particle acceleration and resulting  $\gamma$ -ray emission of SNRs which are presumed to be the sources of the Galactic Cosmic Rays. We first discuss diffusive shock acceleration in shell-type SNRs. Observational upper limits are compared with theoretical predictions for the  $\gamma$ -ray flux and found to be roughly consistent. As a next step the empirical arguments from the observations of X-ray power law continua for Inverse Compton  $\gamma$ -ray emission at TeV energies due to electrons are contrasted to the nucleonic  $\pi^0$  - decay emission from the same objects. Emphasis is given to the possible problems for VHE  $\gamma$ -ray production due to the environmental conditions a SN progenitor finds itself in. Finally, a point is made for the simplest case of SNe Ia, expected to explode in a uniform circumstellar medium. In particular the very recently detected Southern Hemisphere remnant of SN 1006 is compared with Tycho's SNR. On the basis of the assumed parameters for the two remnants we argue that the TeV emission from SN 1006 is dominated by Inverse Compton radiation, whereas Tycho could very well be predominantly a  $\pi^0$  - decay  $\gamma$ -ray source.

## 1. Introduction

Shell-type Supernova Remnants (SNRs) have a special significance among expected Galactic  $\gamma$ -ray sources, because only they have a sufficiently large *hydrodynamical energy output* to replenish the dominant nucleonic component of the Cosmic Rays (CRs) in the Galaxy. The arguments are as follows: Except possibly for  $\gamma$ -ray bursts at cosmological distances, SN explosions are the most violent "events" in the Universe. They have the largest single release of mechanical energy  $E_{SN} \sim 10^{51}$  erg, where a mass  $M_{ej}$  between about one and several  $M_{\odot}$  is ejected with a velocity  $V_0 \sim 10^4$  km/sec. Within the Galaxy, assuming a SN rate  $\nu_{SN} \sim 1/30 \text{ yr}^{-1}$  this also implies the largest mean hydrodynamical energy input into the Interstellar Medium (ISM)  $\langle \dot{E}_{SN} \rangle \sim 10^{42} \text{ erg sec}^{-1} > \langle \dot{E}_{StellarWinds} \rangle > \langle \dot{E}_{Pulsars}^{rot} \rangle$ ; the factors between each of these energy inputs may very well reach values of the order of ten.

Nevertheless  $\langle \dot{E}_{SN} \rangle$  is still only marginally sufficient to replenish the CRs against their escape from the Galaxy  $\langle \dot{E}_{CR} \rangle = E_c \cdot V_{conf}/t_{esc} = E_c \cdot M_{gas} \cdot c/x = 3 \cdot 10^{40} \text{ erg sec}^{-1}$  for an energy-independent "grammage"  $x = 8 \text{ g cm}^{-2}$ , as derived from the CR composition at GeV energies. In this relation  $V_{conf}$  and  $M_{gas}$  denote the CR confinement volume and the interstellar gas mass, respectively. The grammage  $x$  decreases with increasing particle energy as suggested by the observed energy dependence of the CR secondary to primary ratio  $x = 6.9 \cdot (R/20 \text{ GV})^{-0.6} \text{ g cm}^{-2}$  (e.g. Swordy et al., 1990), with  $R = E/Ze$  denoting rigidity, as well as by CR propagation

theory (Ptuskin et al. 1997). Therefore the CR *source spectrum* is significantly harder than the steady state particle spectrum observed near the solar system. This increases the CR energy input requirement from the conventionally estimated few percent of  $\langle \dot{E}_{\text{SN}} \rangle$  (e.g. Berezhinsky et al., 1990) to  $\langle \dot{E}_{\text{CR}} \rangle \sim 1.5 \cdot 10^{41} \text{ erg sec}^{-1}$ , i.e. to something between 10 and 20 percent of  $\langle \dot{E}_{\text{SN}} \rangle$  (Drury et al. 1989). Thus, energetically there are no plausible sources for the CR nucleon component in the Galaxy other than SNRs, and their particle acceleration ought to be very efficient. The same argument does not hold for the CR electrons whose energy density is lower by 2 orders of magnitude at energies exceeding  $\sim 1 \text{ GeV}$ . Therefore the physical nature of the electron sources is energetically much less constrained than that of the CR nucleons.

Apart from the SNR energetics there are quite strong arguments from *acceleration theory*. The energization of nonthermal particles in SNRs is usually assumed to be due to diffusive shock acceleration at the outer shock that sweeps up the circumstellar medium during the expansion of the remnant (for reviews of diffusive shock acceleration theory, see e.g. Drury, 1983; Blandford and Eichler, 1987; Berezhko and Krymsky, 1988; Jones and Ellison, 1991). All models agree that a hard, power law-type nucleon spectrum with maximum energies around 100 TeV should be produced during the evolution of a typical SNR in a diffuse Interstellar Medium (ISM) of not too high density. We shall evaluate the models, as they have been developed to date, in the next section.

Theoretical estimates of the  $\pi^0$  - decay  $\gamma$ -ray luminosity of SNRs (Drury et al., 1994; Naito and Takahara, 1994) have led to the conclusion that the resulting  $\gamma$ -ray flux would be *difficult to observe with present instruments*. We shall discuss the recent TeV searches in the Northern Hemisphere and compare the model predictions with the upper limits.

*Electron acceleration* in SNRs is more difficult to estimate quantitatively since the injection efficiency and even the very process of acceleration for electrons are as yet much less clearly determined. On the other hand, it is empirically plausible that electrons are copiously accelerated in SNRs. For example, the well-known correlation between the integrated Far Infrared and radio continuum luminosities of late type galaxies is dominated by SN precursor stars. The Far Infrared emission is due to dust reradiation of the stellar UV emission. The radio continuum is mainly Synchrotron emission by  $\sim 10 \text{ GeV}$  diffuse galactic CR electrons. It is consistent with a hard source spectrum of CR electrons  $\propto E^{-2}$  and a  $\sim 10^{-2}$  acceleration efficiency ratio of electrons to nucleons (Lisenfeld et al., 1996). In addition, several individual SNRs show X-ray continua which have been attributed to nonthermal Synchrotron emission by multi-TeV electrons (e.g. Koyama et al., 1995). The corresponding Inverse Compton (IC) emission might therefore be able to swamp the nucleonic  $\gamma$ -ray emission from SNRs.

Altogether, real SNRs are not the ideal spherically symmetric configurations as theoreticians tend to picture them for simplicity. The circumstellar environment into which a Supernova explodes can in fact be quite complicated and we shall at least qualitatively attempt to evaluate the effects of these uncertainties.

At the Durban ICRC just before this workshop the Cangaroo group has announced the detection of the Southern Hemisphere SN 1006 in TeV  $\gamma$ -rays. This is a tremendously exciting result which suggests that SNRs are indeed capable to accelerate multi-TeV electrons, as expected from the ASCA observations in the hard X-ray region. Why should then not multi-TeV nucleons be accelerated efficiently as well? We may again use the theoretical estimates for nucleon acceleration, given a set of assumed parameters for this object that have been derived from observations in different wavelength regions. Then it appears that the observed TeV  $\gamma$ -ray flux could be produced in hadronic interactions only with considerable difficulties (!).

This seemingly paradoxical result, when seen in the light of the non-detection of other nearby SNRs in the Northern Hemisphere, can be rationalized if we assume that SN 1006 is an IC  $\gamma$ -ray source. This conclusion is of course highly provisional and needs further careful scrutiny. Tycho's SNR, even though considerably younger, might have a similar  $\pi^0$  - decay flux as SN 1006. If Tycho's X-ray spectrum has only a very small nonthermal component as suggested by the dominance of emission lines, it might indeed be possible to detect its  $\gamma$ -ray emission of hadronic origin in a deep observation with present instruments like the HEGRA stereoscopic system, or Whipple and CAT. The results should be known relatively soon.

## 2. Shock Acceleration in Supernova Remnants

### 2.1. Test Particle Models

The simplest models treat CRs as test particles in a prescribed, time-dependent substrate given by a hydrodynamic solution for the explosion dynamics, for example a Sedov solution. In the first concrete estimates (Cesarsky and Lagage, 1981; Ginzburg and Ptuskin, 1981; Lagage and Cesarsky, 1983) it was assumed that the outer SNR shock was locally plane. With the pitch angle scattering mean free path  $\lambda_{\text{mfp}}(p) = r_{\text{gyro}}(p)$  at the Bohm limit (which implies that a particle is turned around in its motion parallel to the mean magnetic field after each gyration), an upper limit to the achievable maximum momentum  $p_{\text{max}}$  could be calculated by equating  $\tau_{\text{acc}}(p_{\text{max}}) = \text{SNR age}$ .<sup>1</sup> Here

$$\tau_{\text{acc}} = \frac{3}{u_1 - u_2} \left( \frac{\kappa_1}{u_1} + \frac{\kappa_2}{u_2} \right)$$

, with  $\kappa = 1/3 \cdot w \cdot \lambda_{\text{mfp}}$  denoting the diffusion coefficient in the upstream (1) and downstream (2) region, respectively; the particle speed is given by  $w$  (e.g. Drury, 1983). For typical values of the SNR parameters one obtains in this manner  $p_{\text{max}} \sim 10^{14} \text{eV}/c$ .

The actual *nucleon* spectrum in SNRs has first been approximately calculated in the so-called "Onion shell" models (Bogdan and Völk, 1983; Moraal and Axford, 1983): The spectral index  $q(t) = 3r(t)/(r(t) - 1)$  of the accelerated particles at the shock varies with time, following the time dependence of the shock compression ratio  $r(t)$ . To simplify the time dependence of the solution, time is divided into  $n$  intervals and at each time  $t_k$  ( $k = 0, 1, 2, \dots, n$ ) an imaginary shell surface with radius  $R(t_k)$  is created. The  $k^{\text{th}}$  shell contains the material between the shock radii  $R(t_{k-1})$  and  $R(t_k)$ . After being accelerated "at time  $t_k$ ", the particles in a given radial shell  $k$  remain confined *inside* the expanding SNR and therefore loose energy adiabatically. In this kinematic, quasi-stationary model, the maximum particle energy depends on the strength of the shock at  $t = t_k$  and the actually calculated wave spectrum at this time (Völk et al., 1988). To obtain the spatially integrated spectrum inside the SNR at time  $t$ , all shells  $k$  with  $t_k < t$  are summed up. Particles are finally assumed to be released from their SNR source when the shock velocity  $\dot{R}(t)$  decreases below the Alfvén velocity  $v_A \sim 30 - 100 \text{ km sec}^{-1}$  of the ambient medium.

---

<sup>1</sup>In reality, the mean free path will somewhat exceed the gyro radius and therefore  $p_{\text{max}}$  will be smaller than the above estimated value. However, a very strong shock should lead to such strong excitation of scattering MHD waves by the accelerating particles themselves (Bell, 1978; McKenzie and Völk, 1982), that the Bohm limit may indeed approximately be reached in such a system.

The interesting result was that the final source spectrum corresponds approximately to a *single power law* in momentum  $\propto p^{-q_{eff}}$  with  $4.1 \leq q_{eff} \leq 4.3$  over a large range in particle momenta above the injection momenta (Fig. 1). At the end of the so-called sweep-up phase, when the remnant has swept up an amount of interstellar material comparable to the ejected mass from the explosion, the spectrum is very hard  $\propto p^{-4}$ , with the maximum particle energies achieved. After the end of the Sedov phase, the spectrum is softer, with the maximum energy  $cp_{max}$  only slightly exceeding  $10^4$  times the proton rest energy  $mc^2$  for the particular parameters of a Hot ISM. In such a test particle picture the fraction of injected particles  $\delta \sim 10^{-3}$  has to be restricted to smaller values during early times  $t$  in order to not violate total energy flux conservation since no backreaction of the accelerated particles is assumed in such models .

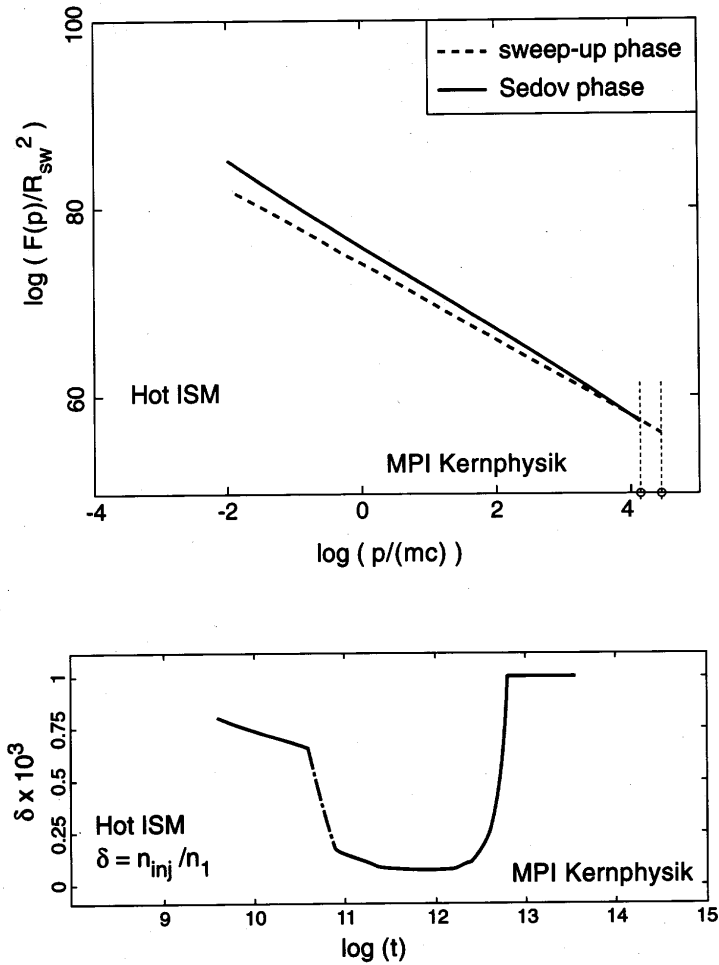


Fig. 1: Test particle model for the overall (spatially integrated) proton momentum spectrum  $F(p)$  (in arbitrary units) of a SNR in a Hot ISM as a function of momentum  $p$  at the end of the sweep-up phase (dashed curve) and at release, i.e. at the end of the Sedov phase (solid line). At sweep-up the spectrum is still quite hard and the upper cutoff higher than at release, when the spectrum is softer due to continued acceleration of low energy particles. In order to conserve total energy flux, the injection rate  $\propto \delta$  must be lowered throughout the early times  $t$  of the evolution (adapted from Völk et al. 1988).

For *electrons* the determination of  $p_{max}$  has to be modified, since it may be determined by

*energy loss processes* rather than by the system age  $t$  alone, as for nucleons. Thus  $\tau_{acc}^{el}(p_{max}) = \text{Min}\{t, \tau_{loss}(p_{max})\}$  (Reynolds and Chevalier, 1981).

Reynolds (1996) has applied such models to the X-ray synchrotron emission from SN 1006. He parametrized the scattering mean free path by a factor  $\eta > 1$  times the electron gyro radius, and introduced the speculative possibility of particle escape from the remnant at some maximum energy. With these additional parameters in the model he argued that the observed X-ray continuum emission from SN 1006 could be explained by the acceleration of electrons up to 100 TeV in the remnant blast wave.

A drastic simplification of the Onion Shell model for electrons was recently made by Maticiadi (1996): he assumed the accelerated particles at any given time to be distributed uniformly over the remnant interior, subject to subsequent adiabatic energy losses. Taking also the magnetic field strength to be uniform inside the remnant and restricting the injection rate by globally requiring an electron to proton ratio of  $10^{-2}$  at release, he could show that the IC yield of these electrons on the MBR at TeV energies is comparable with the expected  $\pi^0$  - decay emission from the nucleonic component.

Even though these electron models simply ignore the difficulty of injecting electrons into the shock acceleration process, they justify themselves by the fact that multi-TeV electrons seem to be required empirically to explain the X-ray synchrotron emission from a number of SNRs (section 5). It seems clear that we have to reckon with electron IC  $\gamma$ -ray emission in all SNRs.

## 2.2. *Nonlinear 2-fluid Models for Nucleons*

The test particle models discussed above are not only of a kinematic and quasi-stationary character, but they also neglect the fact that the nucleonic component must have a strong dynamical influence on the SNR shock ("backreaction") modifying the acceleration process significantly, if this process is to be efficient in the first place.

A simple hydrodynamic approximation for the time-dependent nonlinear equations for the *coupled dynamics* of the thermal gas (plasma) and the accelerating CRs is the so-called 2-fluid model (Axford et al., 1977, 1982; Drury and Völk, 1981). It consists in taking the kinetic energy moment of the CR transport equation and introducing the CR pressure gradient force into the momentum balance for the overall system of plasma and CRs. Extending this fluid approximation to a 3-fluid model (McKenzie and Völk, 1982), also the scattering wave energy can be selfconsistently included. Nonlinear shock modification then leads to the following effects (Fig. 2): In the frame of the shock, the pressure  $p_c$  of the accelerating particles has a gradient that decelerates the incoming flow in the precursor, before the gas pressure, the mass velocity and the mass density finally jump to their downstream values in a subshock. Acceleration is the more efficient the more the shock is smoothed out since in this case irreversible gas heating is reduced and a higher fraction of the free flow energy must go into CR energy. The total compression ratio exceeds the canonical value of 4 and therefore at high energies where the diffusion length is large, the spectrum of accelerated particles is expected to be harder than  $\propto p^{-4}$ , as has been pointed out by Eichler (1984) and Ellison and Eichler (1984) in their kinetic discussion of nonlinear shocks. In a SNR this should be the case during the early evolutionary phases when shock modification is strong.

Particle diffusion into the upstream medium excites hydromagnetic waves there. They propagate against the incoming flow with the Alfvén speed and get further amplified at the (sub)shock. An important aspect is that only these selfexcited waves permit efficient acceleration since

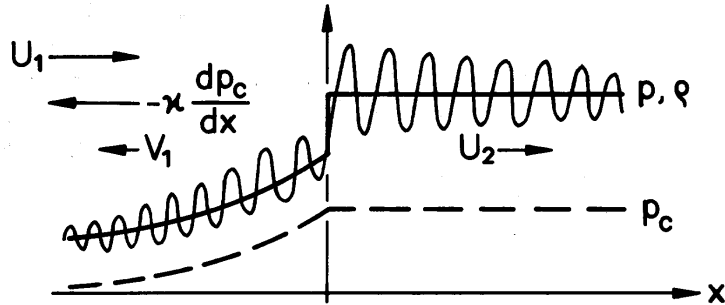


Fig. 2: Nonlinear effects of accelerated particles as seen in the shock frame. The particle pressure gradient  $dp_c/dx$  produces an upstream precursor in gas density  $\rho$  and pressure  $p$ . The diffusion current  $\propto -\kappa dp_c/dx$  excites MHD waves of velocity  $V_1$  which are swept back and amplified in the subshock at the origin.

SNR shocks have a short life-time, typically of the order of  $10^4$ yr; the much weaker average ISM hydromagnetic turbulence alone would make this process basically ineffective.

The hydrodynamic approximation has been applied to SNRs in various forms (Drury et al., 1989; Markiewicz et al., 1990; Dorfi, 1990, 1991; Kang and Jones, 1991). All assume the shock normal to be parallel to the external magnetic field (parallel shock), in an otherwise spherically symmetric configuration. This includes adiabatic energy losses in the remnant interior and diffusive "losses" of particles from the shock into the interior. Obviously none of these effects can be taken into account in an application of plane shock theory to such a configuration. Also heating of the thermal gas by the dissipation of the selfexcited Alfvén waves has been included, even though the diffusion coefficient was maintained at the Bohm limit. This is no contradiction in the limit of strong wave excitation.

Such model calculations show that for very reasonable injection rates 10-30 percent of the entire hydromagnetic SN energy  $E_{SN}$  can be readily converted into CR nuclei during the early evolutionary stages, when the SNR shock is strong. The ultimate release of CRs into the ISM is determined by escape and the details of adiabatic cooling during the late phases where the radiative cooling of the thermal gas and the external pressure compete in decelerating the remnant expansion. However, simple estimates and the numerical results of Dorfi (1991) indicate that an efficiency of CR release of about 10 percent is quite possible.

Even though the hydrodynamic fluid models constitute a simple means to calculate the SNR dynamics including CR production, they do not determine the energy spectra and their temporal evolution. The resulting knowledge of the instantaneous shock compression ratio says little about the overall spectrum, integrated over the remnant interior, which is relevant for the resulting  $\gamma$ -ray spectra.

From a quite different angle, such spectra have been estimated by Baring et al. (1997a) using the Monte Carlo approach to particle scattering of Ellison and Eichler (1984). This is a plane parallel approximation for steady shocks and has a kinematic character, assuming the overall dynamics of the system to be determined in an independent fashion. It is therefore no surprise that the estimated spectra can only give a qualitative indication of the true situation of a dynamical system of basically spherical symmetry. The results were also presented at this workshop by Baring et al. (1997b). Their emphasis is on  $\gamma$ -ray cutoffs and the  $\gamma$ -ray spectral curvature due to the hardening of the spectrum for successively higher energy particles.

### 2.3. Dynamical Kinetic Models

The first nonlinear and fully time-dependent kinetic models for particle acceleration in SNRs have been presented by Berezhko et al. (1994). These authors numerically solved the full combined dynamics of thermal plasma and CRs, using a phenomenological injection model and the Bohm limit for the scattering mean free path. The only limitation of this calculation is the assumption of a parallel shock everywhere, despite the restriction to spherical symmetry. Such an approximation clearly cannot describe asymmetries like that of the X-ray continuum emission from SN 1006. Whether a calculation of the full angular dependence might even imply dynamical instabilities due to the variations in injection rate and acceleration efficiency with angle is unknown. In the following discussion we shall ignore this potential difficulty and assume spherical symmetry.

The resulting solutions show strong shock modifications with increased compression ratios, and highly efficient nucleon acceleration for moderate injection rates. The CR spectra at the shock are hardening towards higher energies. The *spatially integrated overall SNR spectrum at late times* is again an approximate single power law  $\propto E^{-q_{eff}}$ , but harder than the corresponding test particle spectra, since now  $q_{eff} \simeq 4.1$ . We shall apply this model to the  $\gamma$ -ray emission of SNRs in the next section.

## 3. Nuclear $\gamma$ -rays from $\pi^0$ - decay

### 3.1. Hydrodynamic Approximation

The first detailed calculation of the  $\gamma$ -ray emission from SNRs is due to Dorfi (1991). He applied the 2-fluid model, adopting the  $\pi^0$  - decay  $\gamma$ -ray emissivities appropriate for the observed nucleon spectrum in the ISM from Higdon and Lingenfelter (1975), for the 100 MeV energy region. The result was that the  $\gamma$ -ray fluxes from nearby SNRs at  $\sim 1$  kpc distance were near the lower limit of detectability by the COS-B satellite.

Using simplified 2-fluid models for the particle acceleration, Drury et al. (1994, referred to as DAV in the following) also calculated the  $\gamma$ -ray emission, concentrating on the variations with energy and discussing in particular the background problems for its detection (see also Naito and Takahara, 1994). DAV derived the emissivities for various spectral indices  $q_{eff}$ , appropriate for the spectra from CR sources, and pointed out that the diffuse galactic  $\gamma$ -ray background emission at energies  $\gg m_\pi c^2$  decreases with an integral spectral index  $\alpha \equiv q - 3 = 1.7$ , corresponding to the diffuse galactic CR energy spectrum, whereas the emission from the sources like SNRs should decrease considerably slower, with  $\alpha$  between 1.1 and 1.3, according to the test particle results. They concluded that observations of SNRs against the strong diffuse galactic  $\gamma$ -ray background should best be done in the TeV region of currently operating imaging atmospheric Cherenkov telescopes (IACTs). At energies above 100 MeV, corresponding to satellite instruments like COS-B or even EGRET, the  $\pi^0$ - decay  $\gamma$ -ray emission from SNRs would as a rule be drowned in the diffuse Galactic background which also would explain the unsuccessful search for SNRs in  $> 100$  MeV  $\gamma$ -rays so far (Lebrun et al., 1985; Bhat et al., 1985); unfortunately this is still true today despite repeated efforts in this direction (e.g. Osborne et al., 1995).

It was also pointed out that also in the TeV range a detection would be difficult, even for the best present instruments. Their critical parameter is

$$A = \Theta \cdot \left(\frac{E_{SN}}{10^{51}\text{erg}}\right) \cdot \left(\frac{n}{1\text{cm}^{-3}}\right) \cdot \left(\frac{d}{1\text{kpc}}\right)^{-2}$$

,where  $\Theta(t) = E_c(t)/E_{SN}$  denotes the fraction of total SN energy that is in CRs at any given time during SNR evolution.

Since typically  $\Theta \sim 0.1$ , we have  $A \leq 10^{-1}$  or possibly considerably smaller, even for close-by SNRs. Then the flux is indeed marginal for a typical source that extends over about 1 degree. For  $\Theta E_{SN} = 10^{50}\text{erg}$  and  $d = 1\text{kpc}$ , the flux of TeV  $\gamma$ -rays exceeds  $10^{-12}\text{phcm}^{-2}\text{sec}^{-1}$  at  $n \geq 0.1\text{cm}^{-3}$ . The relatively large angular diameter of SNRs makes them usually *extended sources*, making background rejection by an IACT difficult.

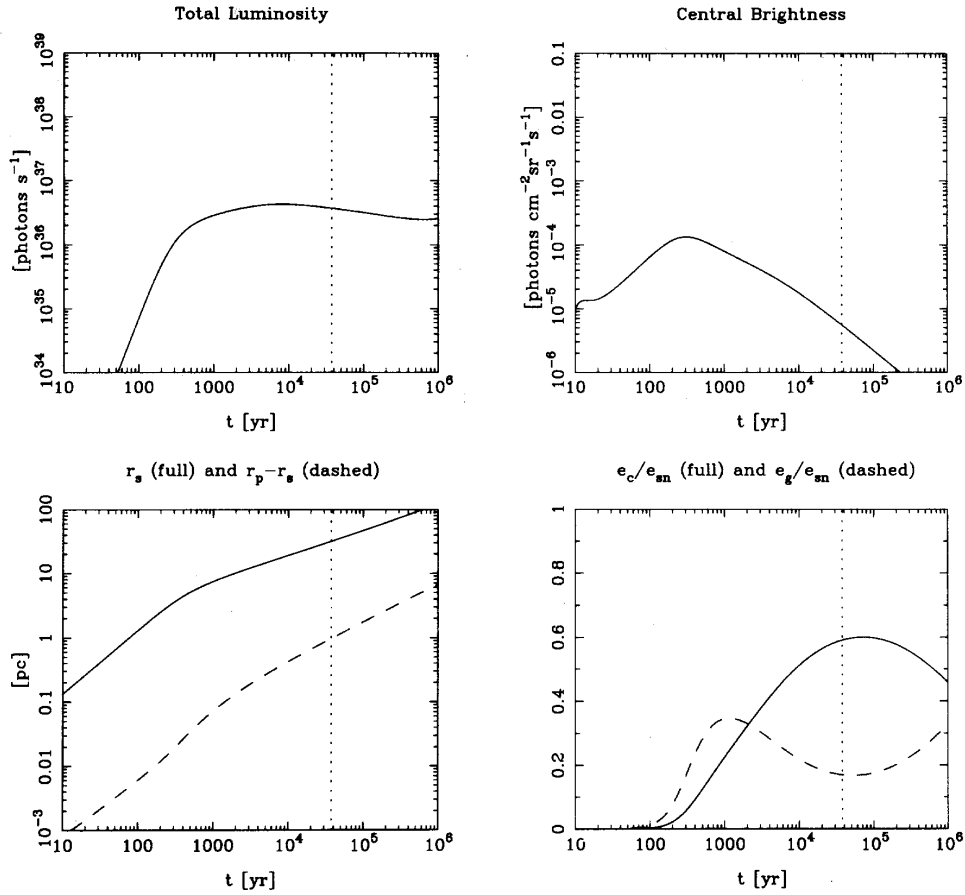


Fig. 3: Two-fluid results for a SNR. The shock radius  $r_s$  increases linearly with time  $t$  until sweep-up, to slow down to and increase  $\propto t^{2/5}$  during the Sedov phase that ends with the onset of radiative cooling (dashed vertical line). The total  $\gamma$ -ray luminosity as well as the total gas ( $e_g$ ) and CR ( $e_c$ ) internal energies increase sharply at sweep-up (cf. Drury et al., 1994).

In calculating the  $\gamma$ -ray emissivity the DAV model effectively assumes that the accelerating particles are distributed *uniformly* across the SNR for all energies. Then the  $\gamma$ -ray energy spectrum is that of a uniform nucleon energy spectrum and for  $E_\gamma \gg m_\pi c^2$  it is proportional to the nucleon spectrum. For the spatially integrated  $\gamma$ -ray luminosity this concentrates all dynamical effects into the single efficiency function  $\theta(t)$  for all  $\gamma$ -ray energies. In general of



course, the particle diffusion length inside the remnant depends on both  $E$  and  $t$ . According to DAV,  $\Theta(t)$  is very small during the sweep-up phase, i.e. for very young SNRs with  $t < t_0 \sim R_0/V_0 \sim (\frac{M_{ej}}{4\pi/3\rho_0})/V_0$ , where  $\rho_0$  denotes the external mass density, and  $V_0$  a characteristic ejecta velocity (Fig. 3). The shock radius  $r_s$  still increases linearly with time in this phase. The  $\gamma$ -ray flux reaches a very flat maximum during the subsequent Sedov phase with a slow decrease thereafter.

### 3.2. Kinetic Theory

The shortcoming of the DAV theory lies in its acceleration aspect. Therefore it is important to substitute the 2-fluid model by a kinetic acceleration model. This has been done by Berezhko and Völk (1997a), based on the theory of Berezhko et al. (1994) described before. In addition, the *distribution of the SN ejecta velocities* (Chevalier and Liang, 1989, and refs. therein) was taken into account. In fact, the fastest ejecta leading the expanding SN material have much higher velocities than those represented by the mean ejecta speed  $V_0 = (2E_{SN}/M_{ej})^{1/2}$ . The very high shock velocities which result from this differential sweep-up at early times  $t < t_0$  increase the acceleration efficiency strongly, with a harder overall proton momentum spectrum at  $t < t_0$  than at  $t > t_0$  (Fig. 4a), and the  $\gamma$ -ray flux rises much faster during the sweep-up phase than in the DAV model at a given  $\gamma$ -ray energy (Fig. 5). At  $t = t_0$  the flux exceeds that of DAV by a factor of several for the same parameters  $n$ ,  $E_{SN}$ , and  $d$  due to a harder particle spectrum, an enhanced CR energy  $E_c$ , and a larger compression ratio relative to the hydrodynamic approximation. On the other hand, after a few times  $t_0$  the kinetic  $\gamma$ -ray flux falls off roughly linearly with time, by a factor of about 10 over a time period 10 times larger than the time of maximum during the subsequent Sedov phase.

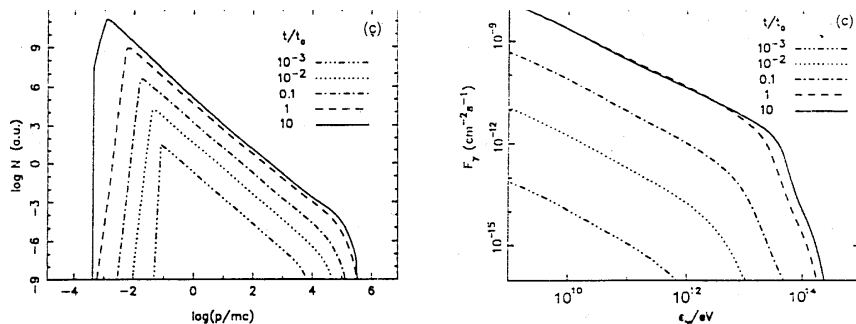


Fig. 4: Overall proton momentum spectrum  $N(p)$  versus  $p/mc$ , for various times in units of the sweep-up time  $t_0$ , in nonlinear kinetic theory (left). The resulting integral  $\pi^0$  - decay  $\gamma$ -ray spectrum  $F_\gamma$  as a function of  $\gamma$ -ray energy  $\epsilon_\gamma$  is shown on the right (from Berezhko and Völk, 1997a).

Mainly this comes from an increasing lack of spatial overlap between the interior CR density with the density increase at the shock for all but the highest particle energies. While the  $\gamma$ -ray observability of a SNR is therefore reduced for times  $t \gg t_0$ , the opposite happens for very young SNRs with  $t < t_0$ . Thus we may be able to detect SNRs approaching the Sedov phase like Tycho's SNR in nuclear  $\gamma$ -rays (see below).

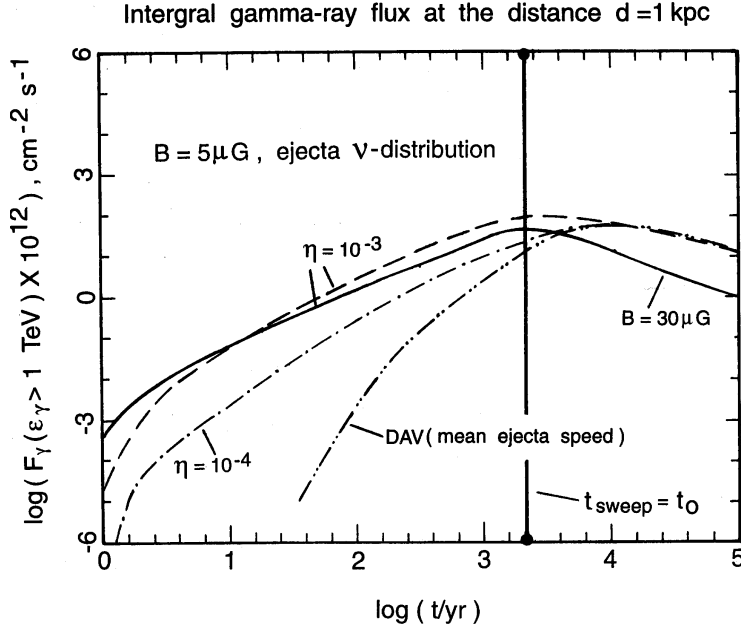


Fig. 5: Temporal evolution of the  $> 1\text{TeV}$   $\gamma$ -ray flux from a SNR in kinetic theory, for various injection rates  $\eta$  and two values of the external field  $B$ , with a distribution of ejecta velocities. This is compared to a 2-fluid model with a single mean ejecta speed (from Berezhko and Völk, 1997a).

The kinetic acceleration theory also allows for the first time the calculation of the integral  $\gamma$ -ray spectrum (Fig. 4b). As expected it hardens with energy similarly to the underlying overall momentum spectrum in the TeV range. The upper cutoff energy rises  $\sim$  linearly with time during sweep-up, and reaches with the Sedov phase a  $\sim$  constant maximum value  $\epsilon_\gamma^{max} \propto n^{-1/3} \simeq E_{CR}^{max}/10 \simeq 10^{13}\text{eV}$  for  $n \simeq 0.3\text{cm}^{-3}$ . This is again assuming the Bohm limit and no escape. If, more realistically,  $\lambda_{mfp} = \eta \cdot r_g(p)$  with  $1 \leq \eta \leq 10$  (e.g. Achterberg et al. 1994), then  $E_{CR}^{max}$  and  $\epsilon_\gamma^{max}$  scale as  $\eta^{-1}$ , without spectral changes for  $\epsilon_\gamma \ll \epsilon_\gamma^{max}$ .

#### 4. Nuclear $\gamma$ -rays and the Observations

When comparing theoretical models for  $\pi^0$  - decay  $\gamma$ -ray emission with recent observations in the TeV range, we shall use the A-parameter while taking into account that the integral spectral index  $\alpha$  is no more a parameter of the theory but in fact quite small,  $\alpha = 1.1$ , or even  $\alpha \leq 1.0$  at  $t \leq t_0$ . Using  $\alpha = 1.1$  for older, and  $\alpha = 1.0$  for very young SNRs, together with  $\Theta = 0.1$ , and  $\Theta = 0.2$ , respectively, corresponds to a conservative theoretical estimate of the nucleonic  $\gamma$ -ray luminosity.

We shall consider here the two SNRs  $\gamma$ -Cygni and IC 443 which have been searched for by the Whipple telescope (Lessard et al., 1997), the Casa MIA (Borione et al., 1995), Cygnus (Allen et al., 1995), and HEGRA AIROBICC (Prah et al., 1997) arrays, and, over parts of the past year, by the HEGRA stereoscopic system of IACTs (Heß et al., 1997). Both sources had been detected by EGRET (Esposito et al., 1996) and due to their location in active star formation regions both are probably the result of the core collapse of massive stars. The data are shown in the upper panel of Fig. 6. The data from the HEGRA CT system are still to be considered preliminary. Both SNRs are extended with a diameter of about 1 degree.

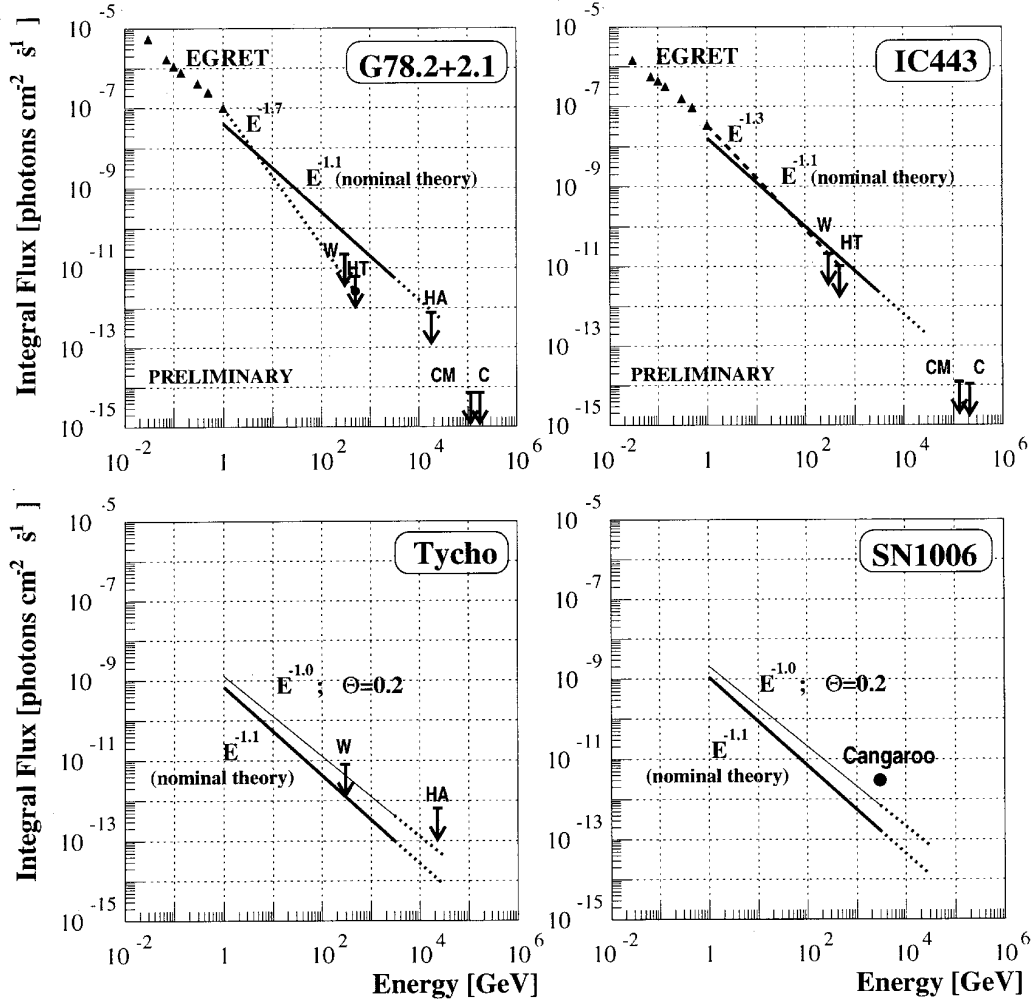


Fig. 6: Data and theoretical predictions for the  $\pi^0$  - decay integral  $\gamma$ -ray flux from 4 nearby SNRs. Data points are from EGRET and Cangaroo. Upper limits (ULs) are from Whipple, the HEGRA stereoscopic system (HT), HEGRA AIROBICC (HA), Casa MIA (CM), and Cygnus (C). The nominal theory corresponds to DAV with an integral spectral index of 1.1, and  $\Theta = 0.1$  (thick line). The thin line has  $\Theta = 0.2$  and spectral index 1.0. The point in the UL of HT for G78.2+2.1 corresponds to the UL from within the EGRET error circle.

	n [cm <sup>-3</sup> ]	E <sub>SN</sub> [erg]	d [kpc]	Θ	α	A
γ-Cygni	5	10 <sup>51</sup>	1.5	0.1	2.1	0.2
IC443	10	2 · 10 <sup>50</sup>	1.5	0.1	2.1	9 · 10 <sup>-2</sup>
SN 1006	0.4	5 · 10 <sup>50</sup>	1.8	0.1	2.1	6 · 10 <sup>-3</sup>
Tycho	1	2 · 10 <sup>50</sup>	2.3	0.1	2.1	4 · 10 <sup>-3</sup>
Cas A	30	10 <sup>51</sup>	3.4	0.1	2.1	0.3

Table 1: Adopted parameters for the 5 SNRs discussed in the text

The EGRET source in γ-Cygni is strongly localized inside the SNR, right at the center of the radio shell, and is geometrically not associated either with a nearby CO cloud (Cong 1977). A physical interaction of the SNR with Cong’s cloud had been suggested by Pollock (1985). If that was indeed the case, Aharonian et al. (1994) would predict a sizeable γ-ray emission from this cloud both at 500 MeV and at 1 TeV. However, Claussen et al. (1997) did not find such an interaction from their OH maser observations at mm wavelengths (as they indeed did for IC 443 and a number of other SNRs).

In Fig. 6 the EGRET data points have been converted to an integral spectrum, together with the upper limits from the observations at much higher energies > 300 GeV and a nominal spectrum with parameters given in Table 1.

The 1 GeV EGRET point would connect to the Whipple and HEGRA telescope upper limits by a hypothetical power law with  $\alpha \sim 1.7$ , much too steep for γ-Cygni to be considered as an accelerating object for VHE Galactic CRs. In fact the EGRET source may rather correspond to a pulsar at this position (see also Brazier et al., 1996). At  $\epsilon_\gamma > 500$  GeV, the HEGRA flux amounts only to about 1/7 of the nominal theoretical flux. This is, unfortunately, still within the uncertainties in the A-parameter that are not determined by acceleration theory. Nevertheless the observed upper limit is uncomfortably low, to be sure.

The case of IC 443 is somewhat different: the spectral index of a power law curve that would connect the HEGRA and Whipple upper limits with the EGRET 1 GeV point has an index of 1.3, only marginally ”too large”. Again it can not be excluded, that the EGRET flux contains the unrelated emission from a pulsar. In other wavelength ranges IC 443 is a complex source that may be even consisting of two SNRs (Asaoka and Aschenbach, 1994). Keohane et al. (1996) discovered a very localized hard X-ray feature using ASCA data, not spatially coincident with the EGRET 95 percent γ-ray detection circle. The SNR interacts strongly with molecular material.

Taking the affected molecular gas together with other parameters for this SNR from Fesen (1984) and Mufson et al. (1986), as well as  $\theta = 0.1$ , we obtain from Table 1 the nominal γ-ray spectrum of Fig. 6.

The Whipple and HEGRA upper limits, at thresholds of 300 and 500 GeV, respectively, lie by the respective factors of 0.7 and 0.6 below the nominal theory, easily within all the uncertainties contained in the A-parameter. We conclude that a deeper observation in the VHE range might indeed lead to a detection even with present instruments. The cases of SN 1006 and Tycho’s SNR will be discussed below.

## 5. Empirical Arguments From X-Ray Power Law Continua

Recent observations of hard X-ray continua from several SNRs with ASCA (SN 1006: Koyama et al., 1995; IC 443: Keohane et al., 1997; RXJ1713.7-3946: Koyama et al., 1997), and RXTE and OSSE (Cas A: Allen et al., 1997; The et al., 1996, 1997) have probably to be interpreted as nonthermal synchrotron emission from VHE electrons with energies ranging up to 100 TeV. These electrons should not all come from pulsars, as the example of SN 1006 shows which is a SN Ia. Thus the energetic electrons should arise from a different process, most likely diffusive shock acceleration. This is also consistent with the radio synchrotron emission from entire galaxies (see Introduction). The difficulty with electrons is that they cannot be easily injected into the shock acceleration process by thermal leakage from the hot downstream region, in an analogous manner as the ions (Levinson, 1994). On the other hand there are many other instabilities associated with shocks that affect electrons. In particular lower hybrid waves have been considered (Galeev, 1984; Galeev et al., 1995, McClements et al., 1997). They might not only pre-energize electrons to be subsequently, for energies  $> 1$  GeV, accelerated by the robust Fermi mechanism along with the nucleons, but they might in addition directly produce nonthermal power laws up to  $10^5$  GeV, as argued by Galeev (1984). Ignoring the latter possibility as less likely, if there are  $> 10$  TeV electrons, there should a fortiori exist many more  $> 10$  TeV nucleons in such SNRs. Kinematic models for electron acceleration in SNRs have been constructed by Reynolds and Chevalier (1981), Ammosov et al. (1994), Reynolds (1996), and Mastichiadis (1996), and have been used to calculate for example the IC emission from SN 1006 (e.g. Reynolds, 1996; Mastichiadis and de Jager, 1996) and W44 (de Jager and Mastichiadis, 1997). Indeed a nonthermal X-ray flux  $F_X$  should be accompanied by an IC  $\gamma$ -ray flux  $F_\gamma = F_X U_{\text{rad}}/U_B$  at the corresponding photon energies  $\epsilon_\gamma \sim h\nu_X \nu_{\text{rad}}/\nu_{\text{gyro}}$ , where  $U_{\text{rad}}$  and  $U_B$  are the energy densities of the radiation field (with characteristic frequency  $\nu_{\text{rad}}$ ) and of the magnetic field, respectively. Time dependent emissions from all radiative processes, given the respective particle populations, have been evaluated by Sturmer et al. (1997) and Gaisser et al. (1997).

## 6. $\pi^0$ - decay vs. IC $\gamma$ -ray fluxes

Despite the low proportion of the electronic nonthermal energy density, the large Thompson cross section and the large number density of MBR photons can lead to an IC component of the TeV  $\gamma$ -ray flux that is quite comparable to that from nucleonic interactions. Nevertheless, for low  $U_{\text{rad}}/U_B$  the synchrotron channel will take over most of the electron energy loss. In addition, for high gas densities the  $\pi^0$  - decay flux will be high. Typically  $U_B$  will be enhanced where the density is enhanced. Thus, in principle, for nuclear  $\gamma$ -rays we should look for SNRs in a high density environment like IC 443 or Cas A. A straightforward pursuit of this approach may however encounter a number of difficulties.

## 7. Problems

We shall here make a short list of possible *reductions* of the  $\gamma$ -ray luminosity relative to the predictions from a blind application of the above model. One case, high ambient densities, has already been mentioned above.

### 7.1. Spherical shocks in a uniform B-field

For a basically spherical SN explosion into a uniform ISM with a homogeneous magnetic field, the shock normal directions will be in general oblique and - in the extreme - even be perpendicular ( $\perp$ ) to the external B-field direction. Thus, first of all, the magnetic compression will vary along the shock surface. Jokipii (1987) has argued that acceleration may be faster for effectively  $\perp$  shocks for  $\eta = \lambda_{\text{mfp}}/r_g = \eta_0 > 1$ , because in this case particle diffusion across the B-field becomes the dominant process for particle transport along the shock normal. However it is not clear at all whether for  $\perp$  shocks scattering waves can also be assumed to be self-excited effectively, and with the right intensity determined by the required parameter  $\eta_0$ . If not, acceleration will be ineffective. Furthermore, for oblique and ultimately  $\perp$  shocks, nucleon injection is increasingly impeded compared to parallel shocks (Bennett and Ellison, 1995; Malkov and Völk, 1995). For all these reasons the nonthermal emission from SNRs will not be spherically symmetric, as clearly visible in the case of SN 1006. For nucleons it would correspond to a reduction in overall acceleration efficiency compared to spherically symmetric models. For shock accelerated electrons the X-ray synchrotron and IC  $\gamma$ -ray lobes of SN 1006 would then occur where the shock is parallel, not where it is perpendicular, in contrast to the assumptions of e.g. Reynolds (1996)! It would be important to measure the polarisation of the X-ray emission, given these contradictory conclusions. Also the intensity distributions should be quite different for the different geometries.

### 7.2. Deviation from the Bohm Limit and High Density

As discussed before, the upper cutoff energy  $E_{CR}^{max} \propto 1/\eta$ . Thus, for  $\eta = 10$  and  $\pi^0$ -decay  $\gamma$ -rays,  $\epsilon_{\gamma}^{max} \simeq 2$  TeV for an external density  $n = 0.3$  (H – atom)  $\text{cm}^{-3}$  (Berezhko and Völk, 1997a). This will not impede observation at energies  $\leq 0.5$  TeV. However, if in addition the external number density is increased by a factor  $\leq 100$  to  $n \leq 30$  (H – atoms)  $\text{cm}^{-3}$ , then  $E_{max} \leq 0.4$  TeV and  $\gamma$ -ray detection at 0.5 TeV threshold is no more possible. Thus a lower threshold  $\sim 100$  GeV becomes a necessary condition as for example envisioned in the HESS and VERITAS projects.

### 7.3. Escape

In an assumed steady state for a strong shock, the necessary existence of an upper cutoff in the momentum distribution implies the escape of particles at this upper cutoff. In a time dependent situation that may not be the case. Nevertheless there might always be a loss of particles at the upper cutoff due to insufficient wave generation there. Another cause for particle losses may be given by purely geometrical conditions, for example in acceleration at a spatially limited shock, like a planetary bow shock in the solar wind. Finally, in a SNR shock the ionization of the upstream circumstellar medium may be insufficient if the gas density is high, despite the ionisation of a radiative precursor by the hot SNR gas. As a result wave damping due to ion-neutral friction may inhibit wave excitation for very high energy particles (e.g. Völk et al., 1981; Draine and McKee, 1993; Drury et al., 1997). Already in moderately dense clouds ( $n \leq 10\text{cm}^{-3}$ ) this implies a cutoff well below 1 TeV.

### 7.4. Magnetic shielding

Gas clouds in the environment of a SNR may be partially shielded if their magnetic field is swept back by the wind from the massive progenitor star. The SNR will then engulf the cloud but not necessarily produce a great intensity of energetic particles that could illuminate

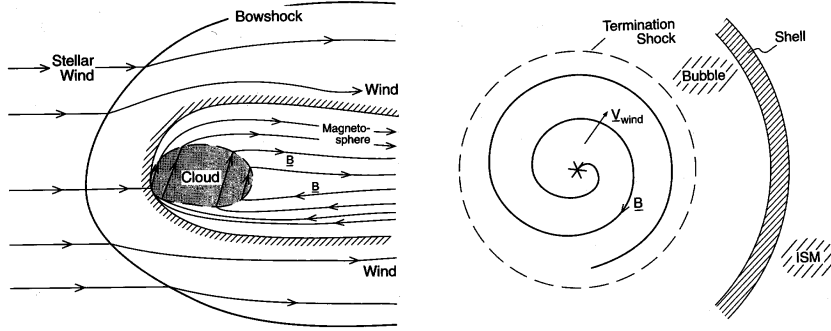


Fig. 7: Flow velocity and magnetic field lines for a supersonic stellar wind around a magnetised interstellar cloud (a). Wind bubble configuration around a rotating massive star. The wind inside the termination shock produces a spiral field configuration. The hot shocked wind in the adjacent bubble compresses ISM material into a dense cold shell separating the bubble from unperturbed ISM (b).

the cloud along the magnetic field lines (Fig. 7a). The shock transmitted into the cloud will be rather slow and may therefore not produce VHE particles while crossing the cloud. Thus, even a physically interacting cloud may not necessarily lead to an enhanced  $\pi^0$ -decay  $\gamma$ -ray luminosity to the extent calculated by Aharonian et al. (1994).

### 7.5. Perpendicular Shock into a Progenitor Wind

If the SN progenitor is a massive star of a mass  $M \sim 20M_{\odot}$ , it will strongly modify its environment by its supersonic mass loss. Combined with the high rotation velocity, the wind will draw out the stellar magnetic field into an Archimedes spiral geometry (Parker, 1958). At a typical distance of  $\sim 1$  pc the radial wind flow will adapt to the exterior pressure in a termination shock beyond which an expanding hot bubble of rarefied shocked stellar wind material creates a dense shell of swept up, cooling interstellar gas (Fig. 7b). The same effect exists for lower mass SN progenitors, but quantitatively it becomes only important for massive stars. When the star subsequently explodes as a SN, particle acceleration will be extremely rapid initially (Völk and Biermann, 1988) due to the high B-field  $\sim 1$  Gauss of stellar origin. Possibly this will be true even at later times (Biermann 1993a, 1993b). Since also the gas density in the wind is very high initially,  $n \propto r^{-2}$ , the  $\pi^0$ -decay  $\gamma$ -ray emission may also be very large at early times as pointed out by Kirk et al. (1995).

The SNR evolution in this complex wind/bubble structure has been modelled in the kinetic approximation (Berezhko and Völk, 1997b), again assuming acceleration at a parallel shock while maintaining overall spherical symmetry. Roughly speaking, the  $\gamma$ -ray luminosity is indeed very large in the wind during an early episode of a few weeks to months, but then it decreases to quite a low value in the shocked wind bubble until the dense shell is reached after  $\sim 10^3$  years. Subsequently the high external gas density leads to a high  $\gamma$ -ray luminosity which persists until the shock weakens and the accelerated particles leave the remnant. The result is a complex time structure of the  $\gamma$ -ray flux as opposed to the case of a SNR in a uniform ISM,

and the observability of such an object will depend critically on the phase of its development. Thus non-detection of such objects in  $\gamma$ -rays at the present time, even though they may look spectacular in other wavelengths, is not a sufficient argument against acceleration. We may have looked at it simply at the wrong time!

However, this is not the whole story yet. In a wind bubble the magnetic field is largely azimuthal except in the very polar regions, near the stellar axis of rotation. Therefore not only injection should be strongly inhibited but possibly also the acceleration itself. The above model calculations should then only constitute an upper limit to the true  $\gamma$ -ray luminosity at any given time. We should perhaps conclude that massive stars (and their demise as SN) which are amongst the most impressive fireworks in the sky, are not necessarily the clearest fingerprints of nonthermal processes in SNRs in general. In addition these SN explosions are likely to leave a pulsar or a black hole behind. Objects like  $\gamma$ -Cygni or IC 443 may well be in this category: too complex and possibly too confused to serve as templates for CR acceleration.

## 8. SNIa in a Uniform Medium

After this complex digression to uncertainties in the theoretical picture and to astronomical difficulties we should now return to comparatively safe grounds. These are SNe in a uniform ISM. SN Ia without obvious interaction with the environment are the natural  $\gamma$ -ray candidates: old stellar objects of low mass, disintegrating completely. Two nearby remnants are of special interest here. SN 1006 has been announced as a detected TeV source by the Cangaroo group during the Durban conference just before this workshop. Tycho's SNR may be a similar object yet with different characteristics, even though only an upper limit exists (Lessard et al., 1997).

### 8.1. SN 1006

Let us first discuss the  $\pi^0$ -decay  $\gamma$ -ray flux. In order to determine the A-parameter we follow Mastichiadis and de Jager (1996, and references therein) who take  $d = 1.8$  kpc,  $E_{SN} = 5 \cdot 10^{50}$  erg, and  $n = 0.4$  cm<sup>3</sup>, which gives  $A = 6.2 \cdot 10^{-3} \cdot (\Theta/0.1)$ , see Table 1<sup>2</sup>. With an integral spectral index  $\alpha = 1.1$  this results in a theoretically predicted flux of  $F_{\gamma,\pi^0}^{\text{th}}(\epsilon_\gamma > 500\text{GeV}) = 1.2 \cdot 10^{-12} \cdot (\Theta/0.1)\text{cm}^{-2}\text{sec}^{-1}$ . Translating this to 3 TeV with a spectral index  $\alpha = 1.1$  gives  $F_{\gamma,\pi^0}^{\text{th}}(\epsilon_\gamma > 3\text{TeV}) = 1.8 \cdot 10^{-13} \cdot (\Theta/0.1)\text{cm}^{-2}\text{sec}^{-1}$ , (Fig. 6). The observed Cangaroo flux is  $F_\gamma^{\text{obs}}(\epsilon_\gamma > 3\text{TeV}) = 3 \cdot 10^{-12}\text{cm}^{-2}\text{sec}^{-1} \simeq 17 \cdot F_{\gamma,\pi^0}^{\text{th}}(\epsilon_\gamma > 3\text{TeV})$ . Since in fact not only the nonthermal X-rays but also the TeV  $\gamma$ -rays appear to come from only parts of the SNR, one might increase the ratio of observed to predicted flux by about 25 percent to a value of about 22. Even though SN 1006 should have essentially reached the Sedov phase, we may nevertheless take  $\Theta = 0.2$  and  $\alpha = 1.0$ , to obtain (in this case) an upper bound of  $F_{\gamma,\pi^0}^{\text{th}}(\epsilon_\gamma > 3\text{TeV}) \simeq 7 \cdot 10^{-13}\text{cm}^{-2}\text{sec}^{-1}$ , (Fig. 6). Reducing this flux by 25 percent, as before, gives  $F_{\gamma,\pi^0}^{\text{th}}(\epsilon_\gamma > 3\text{TeV}) \simeq 5 \cdot 10^{-13}\text{cm}^{-2}\text{sec}^{-1} \simeq (1/6) \cdot F_\gamma^{\text{obs}}(\epsilon_\gamma > 3\text{TeV})$ . Such an upper bound still disregards the possibly higher gas compression ratio between the possibly remaining ejecta and the shock which might exceed that assumed by DAV by a factor up to  $\sim 2$ . Yet this additional factor is not certain and should in any case not explain the above minimum discrepancy by a factor of  $\sim 6$ .

---

<sup>2</sup>The catalog of Greene (1996) quotes a distance range of  $1.7 < d[\text{kpc}] < 3.1$ , a diameter of 30 arc min, and a radio spectral index of 0.6. The uncertainties in the product  $nE_{SN}$  from X-ray data correspond at least to a factor of 2 due to the general difficulties of modelling the *thermal* X-ray emission of SNRs.



Thus, it does not seem possible to explain the observed flux by nucleonic  $\gamma$ -rays without significantly revising the parameters  $n$ ,  $E_{SN}$ , and  $d$ , which are independent of acceleration theory. Of course such a revision can not be excluded, given the uncertainties. On the other hand, the strong nonthermal X-ray emission is suggestive of an IC explanation for SN 1006. This presupposes a fairly low magnetic field, fitted to the radio and X-ray spectra as  $B = 3.5\eta^{2/3}\mu\text{G}$  by Mastichiadis and de Jager (1996), for a gyro factor  $\eta \leq 30$ . Probably  $1 < \eta \ll 10$  and then  $3.5 < B[\mu\text{G}] \ll 16$ . Such low values in a SNR may be entirely possible if we remember that the X-ray emission most likely comes from those regions where the shock normal is roughly parallel to the external magnetic field of several  $\mu\text{G}$ . Using the fit to the radio and X-ray spectra, Mastichiadis and de Jager (1996) applied the simple electron acceleration model of Mastichiadis (1996) to obtain an IC  $\gamma$ -ray flux that roughly agrees with the observed Cangaroo flux provided we choose  $\eta \simeq 3$ , which is an acceptable value.

Clearly, more detailed modelling is needed, but our preliminary conclusion is that SN 1006 is an electron IC source in TeV  $\gamma$ -rays.

### 8.2. Tycho's SNR

This 425 old SNR is probably approaching the end of the sweep-up phase (Tan and Gull, 1985). For an assumed external density  $n \simeq 1\text{cm}^{-3}$ , SN energy  $E_{SN} \simeq 2 \cdot 10^{50}\text{erg}$  (Smith et al., 1988), and distance  $d \simeq 2.3\text{ kpc}$  (Heavens, 1984), one obtains  $A \simeq 4 \cdot 10^{-3}(\Theta/0.1)$ , similar to SN 1006. With  $\alpha = 1.1$  this gives  $F_{\gamma,\pi^0}^{\text{th}}(\epsilon_\gamma > 500\text{GeV}) = 8 \cdot 10^{-13}(\Theta/0.1)\text{cm}^{-2}\text{sec}^{-1}$  which for  $\epsilon_\gamma > 300\text{ GeV}$  lies a factor  $\simeq 6 \cdot (\Theta/0.1)$  below the upper limit of the Whipple observation (Lessard et al., 1997). For  $\alpha = 1.0$  and  $\Theta = 0.2$ , which is an entirely reasonable choice for the evolutionary phase of Tycho, this factor reduces to  $\simeq 1.8$ , and if we would assume a postshock compression ratio  $\sim$  twice that of DAV, Whipple should just have missed a detection of Tycho ! (see Fig. 4)

With an angular diameter of 8 arc min, Tycho's SNR is essentially a point source for TeV  $\gamma$ -ray astronomy with consequent advantages for the  $\gamma$ -hadron separation. If the dominance of emission lines in the X-ray spectrum (Becker et al., 1980; Petre et al., 1993) can be taken as an indication that the nonthermal electron component is very small, then a detection of Tycho's SNR in TeV  $\gamma$ -rays may indeed be the first detection of nuclear  $\gamma$ -rays in a CR source. And there may not be many more such sources in the small sample of nearby candidates available. Thus every effort to find TeV  $\gamma$ -rays in Tycho should be made. At the same time, it is clear that only  $\gamma$ -ray *spectroscopy* together with detailed hard X-ray continuum observations will ultimately enable us to clearly distinguish a  $\pi^0$ -decay source from an IC  $\gamma$ -ray source.

## 9. Conclusions

The conclusions from this discussion can be formulated quite concisely and we will simply do this here:

- SNRs fall into two major categories regarding TeV  $\gamma$ -ray emission
  - SNRS in a uniform ISM and with progenitor masses  $M < 20M_\odot$  are rapidly rising and very slowly decreasing TeV  $\gamma$ -ray sources, except at very high ISM densities, where the upper cutoff energy may not reach present threshold energies of a few hundred GeV, either because the SNR becomes too soon too weak to generate particles of sufficiently high energies, or because the ionisation in the upstream gas is too low to allow strong wave excitation.

- SNRs in wind bubbles of massive progenitor stars  $M > 20M_{\odot}$  should have very low  $\gamma$ -ray emission (except at very early times) until reaching the swept-up shell of interstellar gas. The average magnetic field geometry is unfavourable for efficient acceleration in the first place.
- The theoretical estimates show that it is difficult but not impossible to detect nearby SNRs in  $\gamma$ -rays. These conclusions have been dramatically confirmed by the recent detection of SN 1006. We interpret the present upper limits either as the result of too short observation times (Tycho) or of an unfavourable evolutionary phase in a massive star SNR.
- The ambiguity of an electronic vs. a nuclear origin of the  $\gamma$ -ray emission from SNRs can only be resolved by detailed spectroscopy, both in the TeV and the hard X-ray regions. This observational effort needs to be accompanied by detailed modelling of the synchrotron and IC emission characteristics of the sources.
- As in all other field of astronomy, detailed physics conclusions are only possible in a *multi-wavelength approach*. For SNRs this implies especially a reliable determination of such basic parameters like distance, total explosion energy, and ambient density.

## 10. Acknowledgements

I would like to thank Markus Heß, Evgeny Berezhko, Michail Malkov and Felix Aharonian for informative discussions on SNR physics,  $\gamma$ -ray emission, and acceleration theory.

## References

- Achterberg, A., Blandford, R.D., Reynolds, S.P. 1994, A&A 281,220  
 Aharonian, F.A., Drury, L. O’C., Völk, H.J. 1994, A&A 285, 645  
 Allen, G.E., et al. 1995, ApJ 448, L25  
 Allen, G.E., Geohane, J.W., Gotthelf, E.V., Petre, R., Jahoda, K., Rothschild, R.E., Lingener, R.E., Heindl, W.A., Marsden, D., Gruber, D.E., Pelling, M.R., Blanco, P.R. 1997, to appear in ApJ Letters  
 Ammosov, A.E., Ksenofontov, L.T., Nikolaev, V.S., Pethukov, S.I. 1994, Astron. Lett. 20, 157  
 Asaoka, I., Aschenbach, B. 1994, A&A 284, 573  
 Axford, W.I., Leer, E., Skadron, G. 1977, Proc. 15th ICRC (Plovdiv) 11, 132  
 Axford, W.I., Leer, E., McKenzie, J.F. 1982, A&A 111, 317  
 Baring, M.G., Ellison, D.C., Grenier, I. 1997a, in Proc. 2nd Integral Workshop, ESA, in press  
 Baring, M.G., Ellison, D.C., Reynolds, S.P., Grenier, I., Goret, P. 1997b, (these proceedings)  
 Becker, R.H. et al. 1980, ApJ 235, L5  
 Bell, A.R. 1987, MNRAS 182, 443  
 Bennett, L., Ellison, D.C. 1995, J. Geophys. Res. 100, 3439  
 Berezhko E.G. and Krymsky, G.F. 1988, Sov. Phys. Usp 12, 155  
 Berezhko, E.G., Yelshin, V.K., Ksenofontov, L.T. 1994, Astropart. Phys.2, 215  
 Berezhko, E.G., Völk, H.J. 1997a, Astropart. Phys. 7, 183  
 Berezhko, E.G., Völk, H.J. 1997b, in preparation

- Berezinsky, V.S., Bulanov, S.V., Dogiel, V.A., Ginzburg, V.L., Ptuskin, V.S. 1990, *Astrophysics of Cosmic Rays*, North-Holland Publ. Comp., p. 18ff
- Bhat C.L. et al. 1985, *Nature* 314, 511
- Biermann, P.L. 1993a, *A&A* 271, 649
- Biermann, P.L. 1993b, Proc. 23rd ICRC (Calgary), Invited papers, 45
- Blandford, R.D., Eichler, D. 1987, *Phys. Rep.* 154, 1
- Bogdan, T. and Völk, H.J. 1983, *A&A* 122, 129
- Borione, A. et al. 1995, Proc. 24th ICRC (Rome) 2, 439
- Brazier, K.T.S., Kanbach, G., Carraminana, A., Guichard, J., Merck, M. 1996, *MNRAS* 281, 1033
- Cesarsky, C.J. and Lagage, P.O. 1981, Proc 17th ICRC (Paris) 2, 335
- Chevalier, R.A., Liang, E.P. 1989, *ApJ* 344, 332
- Claussen, M.J., Frail, D.A., Goss, W.M., Gaume, R.A. 1997, to appear in *ApJ*
- Cong, H.I. 1977, Phd thesis, Columbia University
- de Jager, O.C., Mastichiadis, A. 1997, *ApJ* 482, 874
- Dorfi, E.A. 1990, *A&A* 234, 419
- Dorfi, E. 1991, *A&A* 251, 597
- Draine, B.T., McKee, C.F. 1993, *ARAA* 31, 373
- Drury, L.O'C., Völk, H.J. 1981, *ApJ* 248, 344
- Drury, L.O'C. 1983, *Rep. Prog. Phys.* 46, 973
- Drury, L.O'C. Markiewicz, W.J., Völk, H.J. 1989, *A&A* 225, 179
- Drury, L.O'C., Aharonian, F.A., Völk, H.J. 1994, *A&A* 287, 959 (DAV)
- Drury, L.O'C., Duffy, P., Kirk, J.G. 1996, *A&A* 309, 1002
- Eichler, D. 1984, *ApJ* 277, 429
- Ellison, D.C., Eichler, D. 1984, *ApJ* 286, 691
- Esposito, J.A., et al. 1996, *ApJ* 461, 820
- Fesen, R.A. 1984, *ApJ* 281, 658
- Gaisser, T.K., Protheroe, R.J., Stanev, T. 1997, submitted to *ApJ*
- Galeev, A.A. 1984, *Sov. Phys. JETP* 86, 1655
- Galeev, A.A., Malkov, M.A., Völk, H.J. 1995, *J. Plasma Physics* part 1, 54, 59
- Ginzburg, V.L. and Ptuskin, V.S. 1981, Proc. 17th ICRC (Paris) 2, 336
- Heavens, A.F. 1984, *MNRAS* 211, 195
- Heß, M., for the HEGRA Collaboration, 1997, Proc. 25th ICRC (Durban) 3, 229
- Higdon, J.C., Lingenfelter, R.E. 1975, *ApJ* 198, L17
- Jokipii, J.R. 1987, *ApJ* 313, 842
- Jones, F.C. and Ellison, D.C. 1991, *Space Sci. Rev.* 58, 259
- Jones, T.W., Kang, H. 1993, *ApJ* 402, 560
- Kang, H., Jones, T.W. 1991, *MNRAS* 249, 439
- Keohane, J.W., Petre, R., Gotthelf, E.V., Ozaki, M., Koyama, K. 1997, *ApJ* 484, 350
- Kirk, J.G., Duffy, P., Ball, L. 1995, *A&A* 293, L37
- Koyama, K., Petre, R., Gotthelf, E.V., Hwang, U., Matsuura, M., Ozaki, M., Holt, S.S. 1995, *Nature* 378, 255
- Koyama, K., Kinugasa, K., Matsuzaki, K., Nishiuchi, M., Sugizaki, M., Torii, K., Yahauchi, S., Aschenbach, B. 1997, *PASJ* 49, in press
- Lagage, P.O. and Cesarsky, C.J. 1983, *A&A* 125, 249
- Lebrun, F., Paul, J 1985, Proc. 19th ICRC (La Jolla) 1, 309

- Lessard, R.W. et al. 1997, Proc. 25th ICRC (Durban) 3, 233
- Levinson, A. 1994, ApJ 426, 327
- Lisenfeld, U., Xu, C., Völk, H.J. 1996, A&A 306, 677
- Malkov, M.A., Völk, H.J. 1995, A&A 300, 605
- Markiewicz, W.J., Drury, L. O'C., Völk, H.J. 1990, A&A 236, 487
- Mastichiadis, A. 1996, A&A 305, L53
- Mastichiadis, A., de Jager, O.C. 1996, A&A 311, L5
- McClements, K.G., Dendy, R.O., Bingham, J., Kirk, J.G., Drury, L. O'C. 1997, MNRAS in press
- McKenzie, J.F. and Völk, H.J. 1982, A&A 116, 191
- Moraal, H. and Axford, 1983, A&A 125, 204
- Mufson, S.L., McCollough, M.L., Dickel, J.R., Petre, R., White, R., Chevalier, R.A. 1986, Astron. J. 92, 1349
- Naito, T., Takahara, J. 1994, J. Phys. G: Nucl. Part. Phys. 20, 477
- Osborne, J.L., Wolfendale, A.W., Zhang, L. 1995, J. Phys. G: Nucl. Part. Phys. 21, 429
- Petre, R. et al. 1993, in *UV and X-Ray Spectroscopy of Laboratory and Astrophysical Plasmas* (eds Silver, E. & Kahn, S.), Cambridge Univ. Press, 424
- Pollock, A.M.T. 1985, A&A 150, 339
- Prahl, J. and Prosch, C., for the HEGRA Collaboration, 1997 Proc 25th ICRC (Durban) 3, 217
- Ptuskin, V.S., Völk, H.J., Zirakashvili, V.N., Breitschwerdt, D. 1997, A&A 321, 434
- Reynolds, S.P. 1996, ApJ 459, L13
- Reynolds, S.P. and Chevalier, R.A. 1981, ApJ 245, 912
- Smith, A., Davelaar, J., Peacock, A. et al. 1988, ApJ 325, 288
- Sturmer, S.J., Skibo, J.G., Dermer, C.D. 1997, submitted to ApJ
- Swordy, S.P., Müller, D., Meyer, P. L'Heureux, J., Grunsfeld, J.M. 1990, ApJ 349, 625
- Tan, S.M., Gull, S.F. 1985, MNRAS 216,949
- The, L.-S., Leising, M.D., Kurfess, J.D., Johnson, W.N., Hartmann, D.H., Gehrels, N., Grove, J.E., Purcell, W.R. 1996, A&AS 120, 357
- The, L.-S., Leising, M.D., Hartmann, D.H., Kurfess, J.D., Blanco, P., Bhattacharya, D. 1997, preprint astro-ph/9707086
- Völk, H.J., Morfill, G.E., Forman, M.A. 1981, ApJ 249, 161
- Völk, H.J., Zank, L., Zank, G. 1988, A&A 188, 274